

ORCHID: Fairness-Aware Orchestration in Mission-Critical Air-Ground Integrated Networks

Chuan-Chi Lai, *Member, IEEE*, and Chi Jai Choy

Abstract—In the era of 6G Air-Ground Integrated Networks (AGINs), Unmanned Aerial Vehicles (UAVs) are pivotal for providing on-demand wireless coverage in mission-critical environments, such as post-disaster rescue operations. However, traditional Deep Reinforcement Learning (DRL) approaches for multi-UAV orchestration often face critical challenges: instability due to the non-stationarity of multi-agent environments and the difficulty of balancing energy efficiency with service equity. To address these issues, this paper proposes ORCHID (Orchestration of Resilient Coverage via Hybrid Intelligent Deployment), a novel stability-enhanced two-stage learning framework. First, ORCHID leverages a GBS-aware topology partitioning strategy to mitigate the exploration cold-start problem. Second, we introduce a Reset-and-Finetune (R&F) mechanism within the MAPPO architecture that stabilizes the learning process via synchronized learning rate decay and optimizer state resetting. This mechanism effectively suppresses gradient variance to prevent policy degradation, thereby ensuring algorithmic resilience in dynamic environments. Furthermore, we uncover a counter-intuitive efficiency-fairness synergy: contrary to the conventional trade-off, our results demonstrate that the proposed Max-Min Fairness (MMF) design not only guarantees service for cell-edge users but also achieves superior energy efficiency compared to Proportional Fairness (PF), which tends to converge to suboptimal greedy equilibria. Extensive experiments confirm that ORCHID occupies a superior Pareto-dominant position compared to state-of-the-art baselines, ensuring robust convergence and resilient connectivity in mission-critical scenarios.

Index Terms—Air-Ground Integrated Networks, Multi-Agent Reinforcement Learning, UAV Orchestration, Max-Min Fairness, Stability Analysis.

I. INTRODUCTION

As telecommunications evolve toward the Sixth-Generation (6G) era, Air-Ground Integrated Networks (AGINs) have emerged to seamlessly converge terrestrial infrastructure with Non-Terrestrial Networks (NTN), spanning satellites to High Altitude Platforms (HAPs) [1], for ubiquitous global connectivity [2], [3], [4]. Within this heterogeneous architecture, Unmanned Aerial Vehicles (UAVs) play a

This research was supported by the National Science and Technology Council, Taiwan, under Grant No. NSTC 114-2221-E-194-062-. This work was also partially supported by the Advanced Institute of Manufacturing with High-tech Innovations (AIM-HI) from the Featured Areas Research Center Program within the framework of the Higher Education Sprout Project by the Ministry of Education (MOE) in Taiwan. (*Corresponding author: Chuan-Chi Lai*.)

C.-C. Lai is with the Department of Communications Engineering, National Chung Cheng University, Minxiong Township, Chiayi County 621301, Taiwan, and also with the Advanced Institute of Manufacturing with High-tech Innovations (AIM-HI), National Chung Cheng University, Minxiong Township, Chiayi County 621301, Taiwan (e-mail: chuanlai@ccu.edu.tw).

Chi Jai Choy is with the Department of Information Engineering and Computer Science, Feng Chia University, Taichung 407102, Taiwan.

pivotal role as the flexible aerial layer. Serving as agile base stations, UAVs offer rapid wireless coverage extension and mobile edge computing capabilities [5] to complement terrestrial networks [6]. Unlike rigid ground infrastructure, UAVs benefit from high mobility and superior Line-of-Sight (LoS) probabilities. These characteristics enable on-demand coverage for mission-critical scenarios, such as disaster relief operations where ground segments are compromised [7], [8]. In such contexts, establishing a resilient Aerial Access Network (AAN) via collaborative orchestration is not merely a technical enhancement but an absolute necessity to guarantee a reliable *digital lifeline* for trapped or isolated users.

However, realizing collaborative AGINs in public safety scenarios faces two fundamental challenges. The first involves the perceived trade-off between system efficiency and service fairness. Prevalent schemes prioritize maximizing global metrics, specifically the aggregate system sum-rate [9]. While efficient for commercial networks, such strategies are often detrimental in emergency contexts. Maximizing sum-rate biases resources toward users with strong channels, inevitably leading to *coverage starvation* for tail users at the cell edge or obstructed by debris [10]. In mission-critical networks, this creates unacceptable blind spots, failing to provide minimum Quality of Service (QoS) for vulnerable victims. Therefore, fairness in this context is not just a metric of equity but a matter of safety. A “no-user-left-behind” policy is rigorously required to eliminate coverage holes and ensure ubiquitous connectivity [11].

The second challenge stems from the inherent instability of Multi-Agent Reinforcement Learning (MARL). While Deep Reinforcement Learning (DRL) is widely adopted for UAV trajectory design [12], [13], simultaneous multi-agent learning creates a non-stationary environment where optimal policies fluctuate unpredictably. Standard algorithms like MADDPG or MAPPO frequently suffer from primacy bias and policy degradation in late-stage training [14]. Specifically, the accumulation of historical momentum often drives agents into suboptimal local equilibria, making it difficult to adapt to fine-grained coordination requirements. In mission-critical operations, such instability is intolerable; divergence from near-optimal solutions due to excessive variance could compromise infrastructure integrity at a critical moment.

To bridge these gaps, we propose ORCHID (Orchestration of Resilient Coverage via Hybrid Intelligent Deployment), a novel stability-enhanced framework for mission-critical AGINs. First, ORCHID integrates GBS-aware topology partitioning (via modified K-Means++) to mitigate the cold-start

problem, rapidly guiding UAVs toward coarse global optima based on user density [15]. Second, to combat policy degradation, we develop a Reset-and-Finetune (R&F) mechanism. By periodically resetting optimizer states and applying decayed learning rates, R&F enables stable micro-adjustments for precise coverage, effectively resolving the stability-plasticity dilemma. Moreover, distinct from efficiency-first approaches, we formulate a Fairness-Aware objective incorporating Jain's Fairness Index (JFI) to explicitly penalize coverage holes.

The main contributions are summarized as follows:

- **Stability-Enhanced Learning Framework:** We propose the ORCHID framework, a coarse-to-fine orchestration strategy that synergizes GBS-aware initialization with the MAPPO-based R&F mechanism. This two-stage approach effectively suppresses gradient noise and primacy bias, solving the non-stationarity issue inherent in multi-UAV DRL.
- **Efficiency-Fairness Synergy Discovery:** We conduct a rigorous analysis between Max-Min Fairness (MMF) and Proportional Fairness (PF), uncovering a counter-intuitive insight. Overturning the conventional trade-off assumption, our results demonstrate that ORCHID-MMF achieves superior energy efficiency compared to PF. This indicates that MMF avoids the suboptimal greedy equilibria often encountered by PF in complex user distribution topologies.
- **Superior Pareto-Dominance:** Extensive simulations confirm that ORCHID occupies a Pareto-dominant position compared to state-of-the-art baselines (e.g., MADDPG), achieving a 6.8% gain in Normalized Energy Efficiency (NEE) while maintaining robust service fairness, thereby validating its suitability for resilient digital lifelines.

The remainder of this paper is organized as follows. Section II reviews related work. Section III presents the system model. Section IV details the proposed framework. Section V provides performance evaluation, and Section VI concludes the paper.

II. RELATED WORK

This section reviews the state-of-the-art literature on UAV orchestration, categorized into two dominant paradigms: optimization-based approaches and learning-based frameworks. Additionally, fairness-aware resource allocation is critically discussed to motivate the specific design objectives of the proposed ORCHID framework.

A. Optimization-based Approaches

The joint optimization of UAV placement and trajectory design has been extensively investigated to maximize wireless coverage and network performance. Early approaches were predominantly predicated on geometric models and convex optimization techniques. For instance, circle packing theory was utilized to determine optimal 3D coordinates for UAVs, with the objective of maximizing total coverage area while minimizing transmit power [16], [17], [18]. Similarly, heuristic strategies, such as edge-prior placement algorithms,

were proposed to explicitly enhance connectivity for cell-edge users [19]. Nevertheless, these static deployment strategies often assume simplified channel models and uniform user distributions, which renders them ill-suited for complex urban environments or dynamic disaster scenarios.

To accommodate dynamic constraints, the research paradigm has shifted toward sequential decision-making using iterative algorithms. Methods such as Successive Convex Approximation (SCA) and Block Coordinate Descent (BCD) have been widely employed to tackle non-convex trajectory optimization problems [8], [20]. Recent studies have further integrated emerging technologies, including Non-Orthogonal Multiple Access (NOMA) and Reconfigurable Intelligent Surfaces (RIS), into UAV networks. For example, joint optimization frameworks have been formulated to enhance spectral efficiency in NOMA-assisted and STAR-RIS-assisted scenarios [21], [22]. However, these optimization-based approaches typically rely on Alternating Optimization (AO) techniques, which suffer from prohibitive computational complexity and necessitate perfect Channel State Information (CSI). These limitations significantly hinder their applicability in delay-sensitive, mission-critical missions where real-time adaptability is paramount.

B. Learning-based Approaches

To circumvent the computational latency and CSI dependencies of traditional optimization, Deep Reinforcement Learning (DRL) has gained traction as a robust alternative. Pioneering works have successfully applied DRL to UAV navigation and energy efficiency optimization [23], [24]. However, managing the dimensionality curse in complex multi-UAV scenarios remains a formidable challenge due to the exponential growth of the joint state-action space. Consequently, Multi-Agent Reinforcement Learning (MARL) has become the preferred methodology.

To facilitate cooperative behaviors, the Centralized Training with Decentralized Execution (CTDE) framework has been established as the standard architecture. Algorithms such as Multi-Agent Deep Deterministic Policy Gradient (MADDPG) and Multi-Agent Proximal Policy Optimization (MAPPO) enable agents to share global information during training while executing independent decisions during inference [13], [14]. Recent top-tier studies have successfully applied these frameworks to complex UAV orchestration tasks. For instance, multi-agent DRL has been utilized for distributed trajectory optimization in differentiated service scenarios [25], and MAPPO-based approaches have demonstrated effectiveness for hierarchical resource allocation in aerial computing systems [26]. Furthermore, game-theoretic DRL mechanisms have been developed to jointly optimize power allocation and 3D deployment for throughput maximization [27].

Despite these advancements, a pervasive challenge in MARL-based orchestration is non-stationarity. The simultaneous policy updates of multiple agents often induce environmental instability. A critical oversight in most prior works is the assumption of ideal convergence; they often present only best-performing curves while neglecting the issue of policy

degradation or catastrophic forgetting that frequently occurs in later training stages. In contrast, the framework proposed in this study explicitly addresses this stability gap by introducing a resilient two-stage learning mechanism.

C. Fairness-Aware Resource Allocation

Navigating the trade-off between system efficiency and user fairness presents a fundamental dilemma in wireless networks. Prevalent resource allocation schemes largely prioritize the maximization of aggregate system metrics, specifically the system sum-rate [9]. While this objective maximizes total throughput, it inherently biases resource allocation toward users with favorable channel conditions. In public safety or emergency contexts, this Proportional Fairness (PF) strategy can lead to severe coverage holes, failing to guarantee a minimum Quality of Service (QoS) for vulnerable users.

To rectify this disparity, Max-Min Fairness (MMF) has been proposed as a superior objective. Recent literature has explored adaptive deployment approaches that incorporate fairness metrics, such as Jain's Fairness Index (JFI) [11], to balance traffic offloading [28]. While traffic balancing strategies have shown promise [10], directly optimizing for MMF in non-convex UAV environments remains computationally intractable. Existing literature lacks a comprehensive framework that can simultaneously guarantee high user fairness, maintain acceptable system throughput, and ensure the convergence stability of learning agents. The methodology proposed in this paper explicitly addresses these limitations by integrating a MMF-driven objective within a resilient, stability-enhanced MARL architecture.

III. SYSTEM MODEL AND PROBLEM FORMULATION

This section details the system architecture of the proposed mission-critical air-ground integrated network (AGIN). As illustrated in Fig. 1, the network orchestrates a dynamic swarm of UAVs to collaborate with terrestrial infrastructure, aiming to provide resilient connectivity. We characterize the spatial user distribution, UAV mobility dynamics, channel propagation models, and the underlying communication protocol. Finally, we formulate the joint trajectory design and power control problem with a focus on fairness-aware optimization.

Consider a downlink wireless network deployed within a target geographical area of dimensions $D \times D$. The network infrastructure is heterogeneous, comprising two distinct tiers:

- **Terrestrial Tier:** A fixed Macro Ground Base Station (GBS) is located at the center of the service area to provide seamless basic coverage. The position of the GBS is fixed and denoted as $\mathbf{q}_0 = [D/2, D/2, H_{\text{GBS}}]^T$. The GBS operates with a constant transmit power P_{GBS} to maintain a stable service baseline. Unlike the energy-constrained UAVs, the GBS is connected to the power grid; thus, its energy efficiency is not the primary optimization objective in this study.
- **Aerial Tier:** A fleet of N rotary-wing Unmanned Aerial Vehicles (UAVs), denoted by the set $\mathcal{U} = \{u_1, u_2, \dots, u_N\}$, is deployed to assist the GBS. These

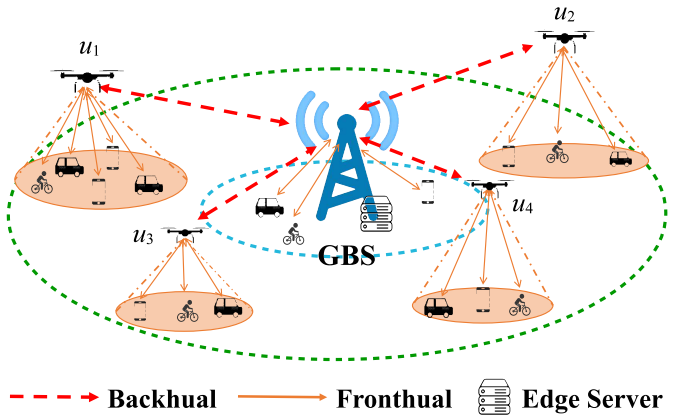


Fig. 1. System model of the hybrid terrestrial-aerial wireless network with multiple UAVs assisting a macro GBS to provide on-demand coverage for ground users.

UAVs act as mobile aerial base stations to offload traffic and enhance coverage for edge users or isolated clusters.

The system serves a set of M Ground Users (GUs), denoted as $\mathcal{G} = \{e_1, e_2, \dots, e_M\}$. The horizontal position of the m -th GU (user e_m) is fixed and known, represented by $\mathbf{x}_m = [x_m, y_m]^T \in \mathbb{R}^2$. The complete 3D coordinate of user e_m is given by $\mathbf{l}_m = [x_m, y_m, 0]^T$, assuming all users are located at ground level ($z = 0$).

A. User Spatial Configuration: Thomas Cluster Process

To accurately reflect the spatial heterogeneity inherent in real-world traffic scenarios (e.g., gatherings in business districts or stadiums), we move beyond the simplistic uniform distribution assumption. Instead, the locations of GUs are modeled using a *Thomas Cluster Process* (TCP) [29], which is a specialized class of Poisson Cluster Processes (PCP).

The generation of user coordinates in TCP involves a two-stage stochastic process:

- 1) **Parent Process (Hotspot Centers):** First, a set of parent points, representing the centers of traffic hotspots, is generated according to a homogeneous Poisson Point Process (HPPP) with intensity λ_p . Let $\Phi_p = \{\mathbf{c}_1, \mathbf{c}_2, \dots, \mathbf{c}_{K_p}\}$ denote the locations of these K_p cluster centers.
- 2) **Daughter Process (User Scattering):** For each parent point $\mathbf{c}_k \in \Phi_p$, a cluster of users (daughter points) is generated. The number of users in each cluster follows a Poisson distribution with mean \bar{M} . The positions of these users are independently and identically distributed (i.i.d.) around the cluster center \mathbf{c}_k following a symmetric bivariate normal distribution with variance $\sigma_{\text{scatter}}^2$.

Mathematically, the probability density function (PDF) of a user's location $\mathbf{x} \in \mathbb{R}^2$ relative to its cluster center \mathbf{c}_k is given by:

$$f(\mathbf{x}|\mathbf{c}_k) = \frac{1}{2\pi\sigma_{\text{scatter}}^2} \exp\left(-\frac{\|\mathbf{x} - \mathbf{c}_k\|^2}{2\sigma_{\text{scatter}}^2}\right), \quad (1)$$

where σ_{scatter} controls the spatial spread of the hotspot. A smaller σ_{scatter} implies highly concentrated traffic, while a larger value indicates a more diffuse hotspot.

Based on this distribution, we adopt a hierarchical service strategy. Users located in the cluster nearest to the map center (i.e., the GBS location \mathbf{q}_0) are associated with the terrestrial tier, forming the set \mathcal{G}_{GBS} . The remaining users, distributed in peripheral hotspots or coverage holes, form the set $\mathcal{G}_{\text{UAV}} = \mathcal{G} \setminus \mathcal{G}_{\text{GBS}}$. The primary focus of this study is the orchestration of the N UAVs to efficiently serve the $M_{\text{UAV}} = |\mathcal{G}_{\text{UAV}}|$ edge users who lack reliable GBS coverage.

B. UAV Mobility Model

The system operates in discrete time steps indexed by $t = 1, 2, \dots, T$, where each time slot has a duration of δ_t . The total mission duration T is constrained by the limited on-board battery capacity of the rotary-wing UAVs.

Let $\mathbf{q}_n(t) = [x_n(t), y_n(t), z_n(t)]^T \in \mathbb{R}^3$ denote the instantaneous 3D position of the n -th UAV (u_n) at time slot t . To ensure compliance with aviation safety regulations and minimize path loss, UAVs are constrained to fly within a designated altitude corridor:

$$H_{\min} \leq z_n(t) \leq H_{\max}, \quad \forall n, t. \quad (2)$$

The mobility of the UAV is modeled using discrete-time kinematics:

$$\mathbf{q}_n(t+1) = \mathbf{q}_n(t) + \mathbf{v}_n(t) \cdot \delta_t, \quad (3)$$

where $\mathbf{v}_n(t)$ represents the velocity vector at time t . The magnitude of the velocity is subject to a mechanical maximum speed constraint, $\|\mathbf{v}_n(t)\| \leq V_{\max}$.

Furthermore, to ensure the physical safety of the aerial fleet, a strict collision avoidance constraint is imposed. The Euclidean distance between any pair of UAVs must maintain a minimum safety clearance d_{\min} at all times:

$$\|\mathbf{q}_n(t) - \mathbf{q}_j(t)\| \geq d_{\min}, \quad \forall n \neq j \in \{1, \dots, N\}, \forall t. \quad (4)$$

C. Channel Propagation Models

The wireless communication environment is characterized by two distinct channel models, corresponding to the terrestrial and aerial links.

1) *UAV-to-User Link (Air-to-Ground)*: For communication between UAVs and GUs, we adopt the probabilistic Air-to-Ground (A2G) channel model proposed in [30]. This model captures the likelihood of Line-of-Sight (LoS) and Non-Line-of-Sight (NLoS) propagation as a function of the UAV's elevation angle.

The probability of establishing an LoS link between UAV u_n and user e_m is given by the sigmoid function:

$$P_{\text{LoS}}(n, m, t) = \frac{1}{1 + a \exp(-b(\theta_{n,m}(t) - a))}, \quad (5)$$

where a and b are environment-dependent S-curve parameters (e.g., representing suburban, urban, or dense urban clutter). The elevation angle $\theta_{n,m}(t)$ (in degrees) is calculated as:

$$\theta_{n,m}(t) = \frac{180}{\pi} \arcsin \left(\frac{z_n(t)}{d_{n,m}(t)} \right), \quad (6)$$

where $d_{n,m}(t) = \|\mathbf{q}_n(t) - \mathbf{x}_m\|$ represents the 3D Euclidean distance between the UAV and the user (assuming the user is at

ground level $z = 0$). The NLoS probability is the complement, $P_{\text{NLoS}} = 1 - P_{\text{LoS}}$.

The associated average path loss (in dB) is formulated as the probabilistic weighted sum of LoS and NLoS components:

$$L_{n,m}^{\text{A2G}}(t) = P_{\text{LoS}} L_{n,m}^{\text{LoS}} + (1 - P_{\text{LoS}}) L_{n,m}^{\text{NLoS}}. \quad (7)$$

Here, the specific path loss for each state $\xi \in \{\text{LoS}, \text{NLoS}\}$ is defined by the free-space path loss (FSPL) augmented by an excessive path loss factor η_ξ :

$$L_{n,m}^\xi = 20 \log_{10}(d_{n,m}(t)) + 20 \log_{10}(f_c) + 20 \log_{10} \left(\frac{4\pi}{c} \right) + \eta_\xi, \quad (8)$$

where f_c is the carrier frequency, c is the speed of light, and η_{LoS} and η_{NLoS} represent the average additional attenuation due to shadowing and scattering in LoS and NLoS conditions, respectively.

2) *GBS-to-User Link (Terrestrial)*: For users served by the GBS, the communication link typically encounters more obstacles than the A2G link. We model this using the log-distance path loss model with large-scale shadow fading. The path loss (in dB) between the GBS and user e_m is expressed as:

$$L_{0,m}^{\text{GBS}}(t) = 20 \log_{10} \left(\frac{4\pi f_c}{c} \right) + 10\gamma \log_{10}(d_{0,m}) + \chi_\sigma, \quad (9)$$

where $d_{0,m} = \|\mathbf{q}_0 - \mathbf{x}_m\|$ denotes the 3D terrestrial distance, γ is the path loss exponent (typically $\gamma \approx 3.5 \sim 4$ for urban ground environments), and χ_σ represents the log-normal shadow fading component, modeled as a zero-mean Gaussian random variable with standard deviation σ_{sh} .

D. Communication Model and User Association

Reliability and interference management are paramount in mission-critical public safety networks. To mitigate severe co-channel interference, we adopt a Frequency Division Multiple Access (FDMA) scheme. The total available bandwidth B_{total} is partitioned into N orthogonal sub-bands of bandwidth $B = B_{\text{total}}/N$, with each sub-band exclusively assigned to a specific UAV. Consequently, inter-UAV interference is efficiently suppressed, allowing the orchestration framework to focus on trajectory and load balancing optimization.

The GBS serves the central user set \mathcal{G}_{GBS} . For edge users in \mathcal{G}_{UAV} , the association follows the Max-RSSI policy. Let $\alpha_{n,m}(t) \in \{0, 1\}$ be the binary association variable, where $\alpha_{n,m}(t) = 1$ if user e_m connects to UAV u_n . The dynamic load (number of served users) of UAV u_n at time t is denoted as $K_n(t) = \sum_{e_m \in \mathcal{G}_{\text{UAV}}} \alpha_{n,m}(t)$.

Unlike the fixed GBS, UAVs perform transmit power control $P_n(t) \in [P_{\min}, P_{\max}]$. The Signal-to-Noise Ratio (SNR) for user e_m served by UAV u_n is:

$$\gamma_{n,m}(t) = \frac{P_n(t) G_{\text{tx}} G_{\text{rx}} 10^{-L_{n,m}^{\text{A2G}}(t)/10}}{\sigma_n^2}, \quad (10)$$

where σ_n^2 represents the thermal noise power.

To model realistic resource contention within each UAV cell, we assume that the bandwidth B is shared equally among the associated users (e.g., via Time Division Multiple Access,

TDMA). Thus, the achievable data rate for user e_m is given by:

$$R_m(t) = \sum_{u_n \in \mathcal{U}} \alpha_{n,m}(t) \frac{B}{K_n(t)} \log_2 (1 + \gamma_{n,m}(t)). \quad (11)$$

This formulation explicitly captures the impact of traffic congestion: as a UAV serves more users (i.e., increasing $K_n(t)$), the per-user data rate decreases. Consequently, the network must inherently balance between maximizing signal strength (proximity) and minimizing service congestion (load balancing) to maintain service quality.

E. Problem Formulation: Multi-Objective Orchestration

The primary objective of this study is to orchestrate the UAV fleet to simultaneously satisfy multiple, often conflicting, service requirements: maximizing user coverage, enhancing spectral efficiency, and ensuring load and rate fairness among edge users. To systematically address these trade-offs, we adopt a weighted sum method to construct a global utility function $U_{\text{total}}(t)$, defined as:

$$U_{\text{total}}(t) = w_1 U_{\text{cov}}(t) + w_2 U_{\text{ee}}(t) + w_3 U_{\text{load}}(t) + w_4 U_{\text{fair}}(t), \quad (12)$$

where w_1, \dots, w_4 are non-negative weighting factors representing the relative priority of each metric.

The utility components capture distinct aspects of network performance. $U_{\text{cov}}(t)$ addresses coverage maximization. Crucially, given the limited battery capacity, we prioritize Energy Efficiency (EE) over raw throughput. The EE utility $U_{\text{ee}}(t)$ is formulated as the ratio of aggregate system throughput to the total transmission power, incentivizing the fleet to provide high-quality service with minimal energy consumption.

Furthermore, to enforce the “no-user-left-behind” policy, we incorporate two fairness-oriented terms: $U_{\text{load}}(t)$ and $U_{\text{fair}}(t)$. These terms apply Jain’s Fairness Index (JFI) to the UAV load distribution and user data rates, respectively, preventing service starvation and ensuring a balanced workload across the aerial fleet.

Let $\mathbf{Q} = \{\mathbf{q}_n(t)\}$, $\mathbf{P} = \{P_n(t)\}$, and $\boldsymbol{\alpha} = \{\alpha_{n,m}(t)\}$ denote the trajectory, power control, and user association variables over the mission horizon T . The joint multi-objective optimization problem is formulated as:

$$(\mathbf{P1}) : \max_{\mathbf{Q}, \mathbf{P}, \boldsymbol{\alpha}} \frac{1}{T} \sum_{t=1}^T U_{\text{total}}(t) \quad (13a)$$

$$\text{s.t. } \|\mathbf{q}_n(t+1) - \mathbf{q}_n(t)\| \leq V_{\max} \delta_t, \quad \forall n, t, \quad (13b)$$

$$\|\mathbf{q}_n(t) - \mathbf{q}_j(t)\| \geq d_{\min}, \quad \forall n \neq j, t, \quad (13c)$$

$$H_{\min} \leq z_n(t) \leq H_{\max}, \quad \forall n, t, \quad (13d)$$

$$\mathbf{q}_n(t) \in [0, D] \times [0, D] \times \mathbb{R}, \quad \forall n, t, \quad (13e)$$

$$P_{\min} \leq P_n(t) \leq P_{\max}, \quad \forall n, t, \quad (13f)$$

$$\alpha_{n,m}(t) \in \{0, 1\}, \quad \forall n, m, t, \quad (13g)$$

$$\sum_{u_n \in \mathcal{U}} \alpha_{n,m}(t) \leq 1, \quad \forall m \in \mathcal{G}_{\text{UAV}}, t. \quad (13h)$$

The optimization is governed by strict physical and operational constraints. The kinematic constraint (13b) limits the

maximum displacement per time slot, reflecting the mechanical speed limit V_{\max} . To ensure flight safety, the non-convex collision avoidance constraint (13c) enforces a minimum separation distance d_{\min} between UAVs. Spatially, the fleet is confined within the designated mission area ($D \times D$) and altitude corridor by constraints (13d) and (13e). Regarding resource allocation, constraint (13f) limits the transmit power to the operational range. Finally, constraints (13g) and (13h) define the user association logic, ensuring that each edge user is served by at most one UAV at any given instant.

F. Problem Complexity

Problem (P1) is a non-convex Mixed-Integer Non-Linear Programming (MINLP) problem. The complexity arises from the coupling of continuous trajectory variables with discrete binary association variables, the non-convexity of the collision avoidance constraints, and the conflicting nature of the multi-objective function. Since deriving a global optimum using traditional convex optimization or exhaustive search is mathematically intractable for large-scale dynamic networks, this necessitates the development of the proposed MARL-based ORCHID framework to find a robust near-optimal solution efficiently.

IV. THE PROPOSED ORCHID FRAMEWORK

In this section, we propose *Orchestration of Resilient Coverage via Hybrid Intelligent Deployment (ORCHID)*, a stability-enhanced two-stage learning framework. As illustrated in Fig. 2, the proposed architecture synergizes unsupervised topology learning with on-policy MARL optimization. This hybrid design enables the UAV fleet to rapidly overcome the exploration cold-start problem and robustly converge to a policy that balances spectral efficiency with the “no-user-left-behind” fairness requirement.

A. Framework Overview

The orchestration process operates in two sequential phases to decouple global partitioning from fine-grained local optimization:

- **Phase I (Initialization):** This phase aims to reduce the high-dimensional exploration overhead of MARL by employing a GBS-Aware Heterogeneous Clustering strategy. Unlike vanilla clustering, it prioritizes user hotspots situated in GBS coverage holes, partitioning the environment into $N + 1$ functional zones. This ensures that the N UAVs are initialized at positions with the highest potential demand, providing a warm-start for the subsequent optimization.
- **Phase II (Resilient Fine-Tuning):** This phase executes a Fairness-Aware MARL Optimization process using a MAPPO-based agent to jointly optimize UAV trajectories and power allocation. To ensure robustness against the non-stationarity of the wireless environment, a *Reset-and-Finetune* mechanism is integrated as a core resiliency feature. By monitoring the JFI stability, the mechanism adaptively resets the optimizer state to maintain convergence and prevent performance degradation even during late-stage policy fluctuations.

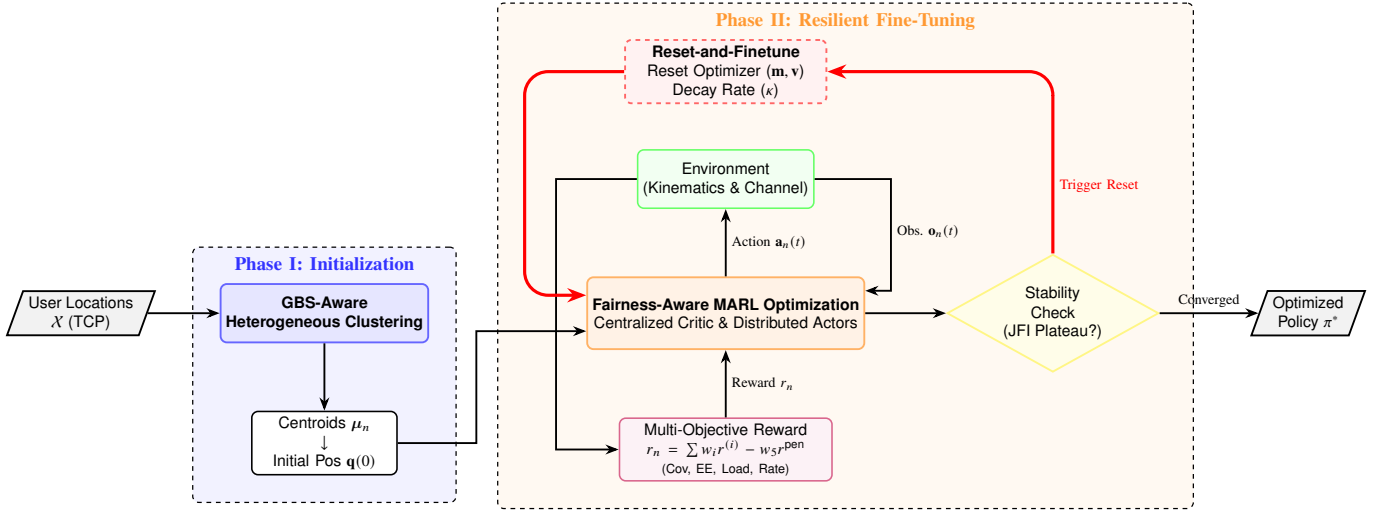


Fig. 2. The overall architecture of the proposed ORCHID framework. The process is divided into two sequential stages: Phase I (Initialization) and Phase II (Resilient Fine-Tuning). In Phase I, a GBS-aware heterogeneous clustering strategy partitions user locations \mathcal{X} into $N + 1$ clusters to define the service scopes for the fixed GBS and N mobile UAVs, providing initial positions for UAV deployment. In Phase II, a Fairness-Aware MARL Optimization is conducted where a MAPPO-based agent dynamically coordinates resource allocation and UAV trajectories. To ensure robustness, a Reset-and-Finetune mechanism monitors the Jain's Fairness Index (JFI) to trigger an optimizer reset (clearing \mathbf{m}, \mathbf{v}) and learning rate decay (by factor κ) whenever a performance plateau is detected.

B. Phase I: GBS-Aware Heterogeneous Initialization

Standard RL algorithms typically initialize agents with random policies. In the continuous coverage control problem, this leads to erratic trajectories and excessive exploration time, known as the *cold-start problem*. To mitigate this, ORCHID leverages the underlying user spatial configuration to perform a GBS-aware initialization.

We formulate the initial deployment problem as a clustering optimization task. Let $\mathcal{X} = \{\mathbf{x}_1, \dots, \mathbf{x}_M\}$ denote the set of horizontal coordinates of all ground users $\mathcal{G} = \{e_1, \dots, e_M\}$. To account for the heterogeneous network structure, we adopt the following partitioning strategy.

First, we perform **Topology Partitioning**. We partition the user set \mathcal{G} into $K = N + 1$ clusters using the K-Means++ algorithm. This minimizes the Within-Cluster Sum of Squares (WCSS), defined as:

$$\text{WCSS} = \sum_{k=1}^{N+1} \sum_{e_m \in C_k} \|\mathbf{x}_m - \boldsymbol{\mu}_k\|^2, \quad (14)$$

where $C_k \subset \mathcal{G}$ represents the subset of users in the k -th cluster, and $\boldsymbol{\mu}_k \in \mathbb{R}^2$ denotes the centroid of cluster C_k .

Next, we apply **GBS Filtering**. We calculate the Euclidean distance between each cluster centroid $\boldsymbol{\mu}_k$ and the fixed GBS location \mathbf{q}_0 (projected to the 2D plane). The cluster centroid nearest to the GBS is identified as the terrestrially served zone and is excluded from the UAV target list.

Finally, we perform **UAV Assignment**. The remaining N centroids determine the initial horizontal coordinates of the N UAVs. Formally, let \mathcal{M}_{UAV} be the set of the N selected centroids. The initial 3D position of the n -th UAV is set as:

$$\mathbf{q}_n(0) = [\boldsymbol{\mu}_n^T, H_{\text{init}}]^T, \quad \forall \boldsymbol{\mu}_n \in \mathcal{M}_{\text{UAV}}, \quad (15)$$

where H_{init} is a pre-configured cruising altitude. This strategy effectively maps the UAVs to the high-density centroids of the

traffic distribution while avoiding redundant coverage over the GBS area.

C. Phase II: Fairness-Aware MARL Optimization

Following the coarse initialization, the problem of fine-grained trajectory design and power control is formulated as a Decentralized Partially Observable Markov Decision Process (DEC-POMDP). We employ the Multi-Agent Proximal Policy Optimization (MAPPO) algorithm, which operates under the Centralized Training with Decentralized Execution (CTDE) paradigm.

1) *Observation and State Spaces*: In the execution phase, each UAV agent $n \in \mathcal{U}$ makes decisions based solely on its local observation $\mathbf{o}_n(t)$. The local observation vector encapsulates the agent's kinematic status, environmental perception, and critical link status:

$$\mathbf{o}_n(t) = \left[\tilde{\mathbf{q}}_n(t), \tilde{P}_n(t), \tilde{d}_{n,\min}(t), \rho_n(t), \mathbf{m}_n(t), \mathbf{v}_n^{\text{viol}}(t), \tilde{\gamma}_n^{\text{BH}}(t) \right]^T. \quad (16)$$

The components are defined as follows: $\tilde{\mathbf{q}}_n(t)$ and $\tilde{P}_n(t)$ are the normalized 3D position and transmit power; $\tilde{d}_{n,\min}(t)$ is the normalized distance to the nearest ground user; $\rho_n(t)$ represents the normalized local served user count; $\mathbf{m}_n(t)$ denotes safety margins relative to boundaries; $\mathbf{v}_n^{\text{viol}}(t)$ tracks historical constraint violations; and $\tilde{\gamma}_n^{\text{BH}}(t)$ is the normalized Signal-to-Noise Ratio (SNR) of the backhaul link to the GBS, enabling the agent to monitor connectivity quality.

During centralized training, the critic network utilizes the global state $\mathbf{s}(t)$, which concatenates all local observations with global context:

$$\mathbf{s}(t) = \{\mathbf{o}_1(t), \dots, \mathbf{o}_N(t), \mathbf{u}_{\text{dist}}, \mathcal{J}(t)\}, \quad (17)$$

where \mathbf{u}_{dist} represents the global distribution of users, and $\mathcal{J}(t)$ is the current global fairness index.

2) *Continuous Action Space*: To enable smooth and precise maneuvering, we employ a continuous action space. The action $\mathbf{a}_n(t) \in \mathbb{R}^4$ for UAV agent u_n is defined as:

$$\mathbf{a}_n(t) = [\Delta\tilde{x}_n, \Delta\tilde{y}_n, \Delta\tilde{z}_n, \Delta\tilde{P}_n]^T, \quad (18)$$

where each component corresponds to the normalized adjustment in the x, y, z coordinates and transmit power, respectively. These values are squashed into $[-1, 1]$ via a tanh activation function. The physical update rule follows:

$$\begin{cases} \mathbf{q}_n(t+1) = \mathbf{q}_n(t) + \mathbf{V}_{\text{scale}} \odot [\Delta\tilde{x}_n, \Delta\tilde{y}_n, \Delta\tilde{z}_n]^T, \\ P_n(t+1) = P_n(t) + \delta_p \cdot \Delta\tilde{P}_n, \end{cases} \quad (19)$$

where $\mathbf{V}_{\text{scale}}$ determines the maximum displacement per step, δ_p is the power adjustment step size, and \odot denotes the element-wise product.

3) *Multi-Objective Reward Mechanism*: To align the agents' behavior with the system objectives, we design a comprehensive reward function. The instantaneous reward $r_n(t)$ for UAV agent u_n at time step t is a weighted sum of four performance metrics and a penalty term:

$$r_n(t) = w_1 r^{\text{cov}}(t) + w_2 r^{\text{ee}}(t) + w_3 r^{\text{load}}(t) + w_4 r^{\text{rate}}(t) - w_5 r_n^{\text{pen}}(t), \quad (20)$$

where w_1, \dots, w_5 are positive weighting factors that balance the relative importance of coverage, energy efficiency, load balance, rate fairness, and safety constraints, respectively.

a) *Coverage Rate* (r^{cov}): To minimize the number of unserved users, this global reward component encourages the fleet to maximize the ratio of covered users:

$$r^{\text{cov}}(t) = \frac{\sum_{u_n \in \mathcal{U}} |\mathcal{G}_n(t)|}{M_{\text{UAV}}}, \quad (21)$$

where $\mathcal{G}_n(t)$ denotes the set of edge users currently served by UAV u_n , and M_{UAV} represents the total number of target users requiring service.

b) *Energy Efficiency* (r^{ee}): To prolong operational endurance, this component incentivizes maximizing the global bit-per-Joule efficiency. The Energy Efficiency (EE) reward is defined as:

$$r^{\text{ee}}(t) = \text{Norm} \left(\frac{\sum_{n=1}^N \sum_{e_m \in \mathcal{G}_n(t)} R_m(t)}{\sum_{n=1}^N P_n(t) + \epsilon} \right), \quad (22)$$

where $R_m(t)$ is the data rate of user e_m , $P_n(t)$ is the transmit power of UAV u_n , and ϵ is a small constant to prevent division by zero. The function $\text{Norm}(\cdot)$ performs normalization (e.g., Min-Max scaling) to map the raw EE value to a stable range suitable for neural network training.

c) *UAV Load Fairness* (r^{load}): To prevent load imbalance among UAVs, we apply Jain's Fairness Index (JFI) to the number of served users $K_n(t) = |\mathcal{G}_n(t)|$:

$$r^{\text{load}}(t) = \frac{\left(\sum_{n=1}^N K_n(t) \right)^2}{N \sum_{n=1}^N K_n(t)^2}, \quad (23)$$

where N is the total number of UAVs in the fleet. This term penalizes configurations where some UAVs are idle while others are overloaded.

d) *UE Capacity Fairness* (r^{rate}): To enforce equitable service quality at the user level, we apply JFI to the users' achieved data rates:

$$r^{\text{rate}}(t) = \mathcal{J}(\mathbf{R}(t)) = \frac{(\sum_{m \in \mathcal{G}_{\text{served}}} R_m(t))^2}{|\mathcal{G}_{\text{served}}| \sum_{m \in \mathcal{G}_{\text{served}}} R_m(t)^2}, \quad (24)$$

where $\mathcal{G}_{\text{served}}$ denotes the subset of users currently receiving service ($R_m > 0$), and $\mathcal{J}(\cdot)$ represents the JFI function.

e) *Constraint Penalties* (r^{pen}): To ensure physical feasibility and connectivity reliability, the penalty term aggregates critical violations:

$$\begin{aligned} r_n^{\text{pen}}(t) = & \omega_c \sum_{j \neq n} \mathbb{I}(d_{nj} < d_{\min}) + \omega_b \mathbb{I}(\mathbf{q}_n \notin \mathcal{B}) \\ & + \omega_{bh} \mathbb{I}(\gamma_n^{\text{BH}}(t) < \gamma_{\text{th}}). \end{aligned} \quad (25)$$

Here, $\mathbb{I}(\cdot)$ is the binary indicator function which equals 1 if the condition is met, and 0 otherwise. The coefficients $\omega_c, \omega_b, \omega_{bh}$ represent the penalty intensities for inter-UAV collision ($d_{nj} < d_{\min}$), boundary overstepping ($\mathbf{q}_n \notin \mathcal{B}$), and weak backhaul connectivity ($\gamma_n^{\text{BH}} < \gamma_{\text{th}}$), respectively.

f) *Optimization Goal (Cumulative Return)*: The ultimate goal of the RL agent is to maximize the expected discounted cumulative return over the mission horizon T :

$$J(\pi_\theta) = \mathbb{E}_{\pi_\theta} \left[\sum_{t=0}^T \gamma^t r_n(t) \right], \quad (26)$$

where π_θ is the policy parameterized by θ , and $\gamma \in [0, 1]$ is the discount factor determining the importance of future rewards.

4) *MAPPO Learning Objective*: To solve this optimization problem, the policy π_θ and value function V_ϕ are updated iteratively. The actor is updated by maximizing the clipped surrogate objective:

$$\begin{aligned} L(\theta) = & \mathbb{E}_t \left[\min \left(\rho_t(\theta) \hat{A}_t, \right. \right. \\ & \left. \left. \text{clip}(\rho_t(\theta), 1 - \epsilon_{\text{clip}}, 1 + \epsilon_{\text{clip}}) \hat{A}_t \right) \right] + \sigma H(\pi_\theta), \end{aligned} \quad (27)$$

where $\rho_t(\theta)$ is the probability ratio between new and old policies, \hat{A}_t is the Generalized Advantage Estimation (GAE), ϵ_{clip} is the clipping parameter to limit policy updates, and σ is the entropy coefficient regulating the exploration-exploitation trade-off via the entropy term $H(\pi_\theta)$.

D. Stability Enhancement: The Reset-and-Finetune Mechanism

A critical challenge in on-policy MARL is *policy degradation* during late training stages [31]. As agents converge towards a local optimum, adaptive optimizers such as Adam accumulate historical momentum from the early exploration phase. This historical inertia can inadvertently drive the policy away from a precise optimum, a phenomenon akin to the *primacy bias* observed in deep RL [32]. To counteract this, ORCHID introduces a formal *Reset-and-Finetune (R&F)* mechanism.

Let \mathcal{J}_e denote the global JFI score at episode e . We quantify the training stability via a sliding window moving average $\bar{\mathcal{J}}_e$ over a window size W :

$$\bar{\mathcal{J}}_e = \frac{1}{W} \sum_{k=0}^{W-1} \mathcal{J}_{e-k}. \quad (28)$$

The *Stabilization Phase* is triggered at episode e^* when the relative performance gain drops below a convergence threshold ϵ_{tol} , indicating a topological plateau:

$$e^* = \min\{e \mid |\bar{\mathcal{J}}_e - \bar{\mathcal{J}}_{e-W}| < \epsilon_{\text{tol}} \cdot \bar{\mathcal{J}}_{e-W}\}. \quad (29)$$

Here, the window size W acts as a temporal filter, allowing the system to distinguish between transient stochastic fluctuations and genuine policy stagnation.

Upon triggering at $e = e^*$, we execute two synchronized operations to enforce a hard transition from global exploration to local exploitation.

a) *Optimizer State Reset*: The standard Adam optimizer maintains the first moment estimate \mathbf{m}_t (momentum) and the second raw moment estimate \mathbf{v}_t (variance). In dynamic UAV coverage, gradients collected during the early high-velocity exploration phase are often uncorrelated with the fine-grained adjustments required in the final stages [33]. We explicitly decouple the optimization trajectory by resetting these internal states for all network parameters:

$$\mathbf{m}_t \leftarrow \mathbf{0}, \quad \mathbf{v}_t \leftarrow \mathbf{0}, \quad \text{at } t = t(e^*), \quad (30)$$

where $t(e^*)$ denotes the time step corresponding to the start of episode e^* . This effectively clears the historical "inertia," forcing the optimizer to respond solely to the local curvature of the current loss landscape.

b) *Synchronized Learning Rate Decay*: Simultaneously, to enable precise micro-adjustments without overshooting the local optimum, the learning rates $\eta \in \{\eta_{\text{actor}}, \eta_{\text{critic}}\}$ undergo a Heaviside step decay:

$$\eta_e = \begin{cases} \eta_{\text{init}}, & \text{if } e < e^* \\ \kappa \cdot \eta_{\text{init}}, & \text{if } e \geq e^* \end{cases}, \quad (31)$$

where κ is the damping factor (set to 0.1 in our implementation). This drastic reduction is theoretically necessitated by the optimizer reset. Without historical momentum to smooth out stochastic gradients, maintaining a high learning rate would introduce severe variance, potentially preventing convergence [34]. Mathematically, by scaling η by κ , the variance of the parameter updates is suppressed quadratically:

$$\text{Var}(\Delta\theta') \approx \kappa^2 \cdot \text{Var}(\Delta\theta) = 0.01 \cdot \text{Var}(\Delta\theta). \quad (32)$$

This order-of-magnitude reduction acts as a numerical damper, effectively locking the UAV fleet into a low-variance equilibrium, thereby validating the robustness of the R&F mechanism.

E. Algorithm Description and Complexity Analysis

The complete training and execution procedure of the proposed ORCHID framework is summarized in Algorithm 1. The process naturally divides into the offline optimization phase and the online execution phase.

Algorithm 1: ORCHID: Two-Stage Orchestration Framework

Input: User Location Set \mathcal{X} , GBS Position \mathbf{q}_0 , No. of UAVs N , Max Episodes E_{max} , Total Steps T , R&F Window Size W , Stability Threshold ϵ_{tol} , Learning Rates $\eta_{\text{actor}}, \eta_{\text{critic}}$, Decay Factor κ .

Output: Optimized Policy π_{θ}^* .

```

/* Phase I: Initialization via
Heterogeneous Clustering */
```

1 Run K-Means++ on user set \mathcal{X} to generate $N + 1$ centroids;

2 Identify centroid μ_{near} closest to \mathbf{q}_0 and discard it (GBS Filtering);

3 Assign remaining N centroids to UAVs:

$$\mathbf{q}_{1:N}(0) \leftarrow \mu_{\text{rem}}$$

```

/* Phase II: Resilient Fine-Tuning
(MAPPO with R&F) */
```

4 Initialize Actor π_{θ} , Critic V_{ϕ} , and Replay Buffer \mathcal{D} ;

5 **for** episode $e = 1$ to E_{max} **do**

6 Reset environment and receive initial state \mathbf{s}_0 ;

7 **for** step $t = 1$ to T **do**

8 Each UAV u_n observes $\mathbf{o}_n(t)$ and executes $\mathbf{a}_n(t) \sim \pi_{\theta}(\cdot | \mathbf{o}_n(t))$;

9 Env transitions to \mathbf{s}_{t+1} and calculates reward $r_n(t)$;

10 Store transition $(\mathbf{s}_t, \mathbf{a}_t, \mathbf{r}_t, \mathbf{s}_{t+1})$ in \mathcal{D} ;

11 **end**

12 /* Policy Update and Stability
Enhancement */

13 Update θ, ϕ using MAPPO objective on batch from \mathcal{D} ;

14 **if** Plateau detected ($|\bar{\mathcal{J}}_e - \bar{\mathcal{J}}_{e-W}| < \epsilon_{\text{tol}}$) **and** not
reset yet **then**

15 Reset Adam optimizer states: $\mathbf{m} \leftarrow \mathbf{0}, \mathbf{v} \leftarrow \mathbf{0}$;

16 /* Synchronized Learning Rate
Decay */

17 $\eta_{\text{actor}} \leftarrow \kappa \cdot \eta_{\text{actor}}$;

18 $\eta_{\text{critic}} \leftarrow \kappa \cdot \eta_{\text{critic}}$;

19 Mark as R&F triggered;

20 **end**

1) *Offline Complexity (Initialization & Training)*: The computational burden is primarily concentrated in the pre-deployment phase. Phase I utilizes the GBS-aware K-Means strategy with a complexity of $O(I \cdot (N + 1) \cdot M)$, where I is the number of iterations and M is the number of users. Since this is a one-off procedure, it introduces zero latency to the mission. In Phase II, the centralized training complexity scales as $O(E_{\text{max}} \cdot T \cdot N \cdot B)$, where B is the batch size for PPO updates. Although extensive, the embedded Reset-and-Finetune operations involve only scalar resets and scaling, adding negligible $O(1)$ overhead. Crucially, both tasks are executed on a powerful centralized server prior to deployment.

2) *Online Complexity (Real-time Inference)*: For dynamic deployment, the critical metric is the inference latency on

onboard processors. Each UAV independently executes a forward pass through its Actor network. With network depth L and width H_l , the decision complexity is $O(\sum_{l=1}^{L-1} H_l \cdot H_{l+1})$. Given our lightweight MLP architecture (e.g., $H = 256$), this operation involves only simple matrix-vector multiplications, which are executable in milliseconds on embedded edge devices.

V. PERFORMANCE EVALUATION

This section validates the effectiveness of the proposed ORCHID framework through comprehensive simulations. We detail the simulation environment, comparative baselines, and the performance metrics used to quantify the system's balance between coverage, throughput, and fairness.

A. Simulation Setup

We simulate a mission area of size $D \times D = 1 \times 1 \text{ km}^2$ containing a central GBS, implemented using Python and PyTorch. Ground user distribution follows the *Thomas Cluster Process* (TCP) described in Section III, generating realistic heterogeneous traffic patterns with distinct hotspots ($K_p = 5$ parent clusters).

The aerial fleet consists of N rotary-wing UAVs operating within a 3D space. The channel model simulates a standard urban environment, incorporating elevation-dependent probabilistic LoS and NLoS links. Regarding resource sharing, we assume an Equal Time Sharing (Round-Robin) scheme within each UAV cell, consistent with (11).

a) *Optimization Objectives (MMF vs. PF)*: To rigorously evaluate the trade-off between service equity and system efficiency, our experiments compare two distinct orchestration objectives:

- **Max-Min Fairness (MMF)**: The default configuration for ORCHID. It prioritizes the "no-user-left-behind" policy by maximizing the Jain's Fairness Index (JFI) in the reward function, ensuring that UAVs actively serve worst-case users.
- **Proportional Fairness (PF)**: A comparative configuration where the agents aim to maximize the sum of logarithmic data rates ($\sum \log R_m$). This typically yields higher aggregate throughput but may tolerate lower rates for edge users.

Unless otherwise specified, the simulations use the MMF configuration.

For the MARL architecture, both Actor and Critic networks utilize Multi-Layer Perceptrons (MLPs) with three hidden layers (256 neurons each, ReLU activation), optimized via Adam with a batch size of 128. To ensure convergence, the R&F mechanism monitors the performance trend over a sliding window to trigger stability phase transitions. Key simulation parameters are summarized in Table I.

As specified in Table I, we employ asymmetric learning rates ($\eta_{\text{critic}} = 10^{-3}$, $\eta_{\text{actor}} = 10^{-4}$) to enhance stability. A higher η_{critic} allows the Critic to rapidly adapt to dynamic interference and provide timely feedback, while a conservative η_{actor} ensures smooth trajectory evolution and prevents drastic policy oscillations.

TABLE I
SIMULATION PARAMETERS

Category	Parameter	Value
Network	Service Area Size ($D \times D$)	$1 \times 1 \text{ km}^2$
	Number of Ground Users (M)	50
	GBS Position (\mathbf{q}_0)	[500, 500, 30] m
UAV	Number of UAVs (N)	6
	Altitude Range [H_{\min}, H_{\max}]	[80, 120] m
	Max Horizontal Speed (V_{\max})	5 m/s
	Transmit Power Range [P_{\min}, P_{\max}]	[100, 200] mW
Channel	Carrier Frequency (f_c)	2.4 GHz
	Sub-band Bandwidth (B)	10 MHz
	Noise Power Density (N_0)	-174 dBm/Hz
Learning	Discount Factor (γ)	0.99
	Actor Learning Rate (η_{actor})	10^{-4}
	Critic Learning Rate (η_{critic})	10^{-3}
	Decay Factor (κ)	0.1
	Batch Size (N_{batch})	128
	R&F Window Size (W)	50

To demonstrate the superiority of ORCHID, we compare its performance against three representative baselines covering static heuristics, traditional optimization, and standard deep reinforcement learning:

- **Static Random Deployment (Lower Bound)**: In this scheme, the UAVs are initialized at random 3D coordinates within the designated mission area and maintain their positions throughout the entire service duration. This baseline represents the most naive deployment strategy, serving as a performance lower bound to quantify the gains achieved by intelligent positioning and dynamic mobility.
- **Static K-Means Clustering (Heuristic)**: This method executes only **Phase I** of our framework (including GBS filtering). The UAVs are deployed to the centroids calculated by the GBS-aware K-Means algorithm and hover at fixed positions for the entire mission duration. This baseline evaluates the necessity of the dynamic fine-tuning phase (Phase II) in handling time-varying channel conditions and enforcing fairness.
- **MADDPG (RL Baseline)**: We employ the Multi-Agent Deep Deterministic Policy Gradient (MADDPG) algorithm [13], a popular off-policy actor-critic method. To ensure a fair comparison, MADDPG is trained with the same multi-objective reward function as ORCHID but utilizes random initialization and standard exploration noise without the proposed R&F stability mechanism.

B. Evaluation Metrics

The system performance is evaluated based on the following three key metrics, averaged over the evaluation episodes:

- 1) *User Coverage Rate*: This metric quantifies the service availability of the network. A user is considered "covered" if their achievable SINR exceeds a minimum service threshold Γ_{req} . The coverage rate is defined as:

$$\text{Coverage} = \frac{1}{T} \sum_{t=1}^T \frac{\sum_{u_n \in \mathcal{U}} |\mathcal{G}_n(t)|}{M_{\text{UAV}}} \times 100\%, \quad (33)$$

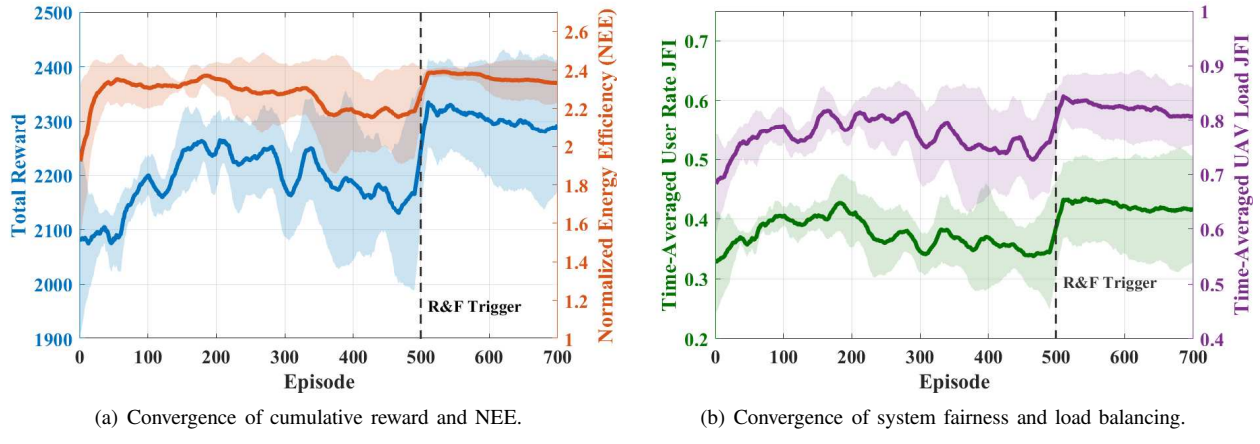


Fig. 3. Training convergence analysis of the ORCHID framework over 700 episodes. Solid lines and shaded areas denote the mean and ± 1 standard deviation over 5 independent runs. The vertical dashed line at $e = 500$ marks the activation of the R&F mechanism, initiating the stability phase.

where M_{UAV} is the total number of target edge users, and $\mathcal{G}_n(t)$ denotes the set of users served by UAV u_n satisfying the SINR requirement.

2) *Normalized Energy Efficiency (NEE):* Given the limited energy budget of UAVs, Energy Efficiency (EE) serves as a paramount performance metric. We focus on the communication efficiency, defined as the ratio of aggregate throughput to the total transmission power. The instantaneous system energy efficiency $\text{EE}_{\text{sys}}(t)$ (bits/Joule) is:

$$\text{EE}_{\text{sys}}(t) = \frac{\sum_{u_n \in \mathcal{U}} \sum_{e_m \in \mathcal{G}_n(t)} R_m(t)}{\sum_{u_n \in \mathcal{U}} P_n(t)}. \quad (34)$$

To strictly quantify the relative performance gains across different operational regimes, we evaluate the Normalized Energy Efficiency (NEE). Specifically, the NEE is calculated by normalizing the time-averaged EE of the proposed method against that of the baseline:

$$\text{NEE} = \frac{1}{T \cdot \overline{\text{EE}}_{\text{random}}} \sum_{t=1}^T \text{EE}_{\text{sys}}(t), \quad (35)$$

where $\overline{\text{EE}}_{\text{random}}$ represents the average energy efficiency achieved by the Static Random Deployment strategy. An NEE value greater than 1.0 indicates a net performance improvement over the lower-bound heuristic.

3) *Fairness and Load Balancing Metrics:* To evaluate the equity of resource allocation over the entire mission duration, we adopt the Time-Averaged Jain's Fairness Index (JFI), extending the instantaneous definitions provided in Section IV-C.

a) *UAV Load Fairness ($\overline{\text{JFI}}_{\text{load}}$):* To assess the workload distribution among the fleet, we compute the time-averaged UAV Load Fairness based on the instantaneous definition in (23), denoted as $r^{\text{load}}(t)$:

$$\overline{\text{JFI}}_{\text{load}} = \frac{1}{T} \sum_{t=1}^T r^{\text{load}}(t). \quad (36)$$

Ideally, $\overline{\text{JFI}}_{\text{load}} \approx 1$ indicates that the workload remains evenly distributed among the UAV fleet during the entire mission, preventing scenarios where some UAVs are overloaded while others are idle.

b) *User Rate Fairness ($\overline{\text{JFI}}_{\text{rate}}$):* Complementing load balance, we evaluate the service consistency experienced by the ground users. Based on the instantaneous User Rate Fairness $r^{\text{rate}}(t)$ defined in (24), the time-averaged metric is:

$$\overline{\text{JFI}}_{\text{rate}} = \frac{1}{T} \sum_{t=1}^T r^{\text{rate}}(t). \quad (37)$$

A higher $\overline{\text{JFI}}_{\text{rate}}$ implies that the network maintains uniform service quality for all users throughout the episode, effectively implementing the “no-user-left-behind” policy.

C. Convergence and Stability Analysis

The training dynamics and stability of the ORCHID framework are evaluated in Fig. 3. As shown in Fig. 3(a), both the Total Reward and Normalized Energy Efficiency (NEE) exhibit a rapid upward trajectory during the initial 100 episodes. This warm-start advantage is primarily attributed to the GBS-aware K-Means initialization (Phase I), which provides an optimized starting topology for the UAV fleet, avoiding the inefficiency of random exploration.

The critical efficacy of the Reset-and-Finetune (R&F) mechanism is vividly demonstrated following the trigger at $e^* = 500$ (indicated by the vertical dashed line). Prior to this point ($e \in [200, 500]$), the system exhibits signs of entrapment in a local optimum, characterized by significant variance and performance plateaus. However, immediately upon entering the *Stabilization Phase*, the Total Reward (blue curve) achieves a distinct performance leap, breaking through the previous ceiling of 2250. Simultaneously, the NEE (orange curve) rapidly converges to its peak value of approximately 2.4 times the random baseline. Notably, the confidence interval of the NEE significantly narrows in this phase, confirming that the synchronized optimizer reset and learning rate decay successfully suppress stochastic noise, locking the policy into a high-performance equilibrium.

The temporal evolution of network equity is illustrated in Fig. 3(b). A compelling observation is the trajectory of the User Rate JFI ($\overline{\text{JFI}}_{\text{rate}}$, green curve). During the pre-trigger

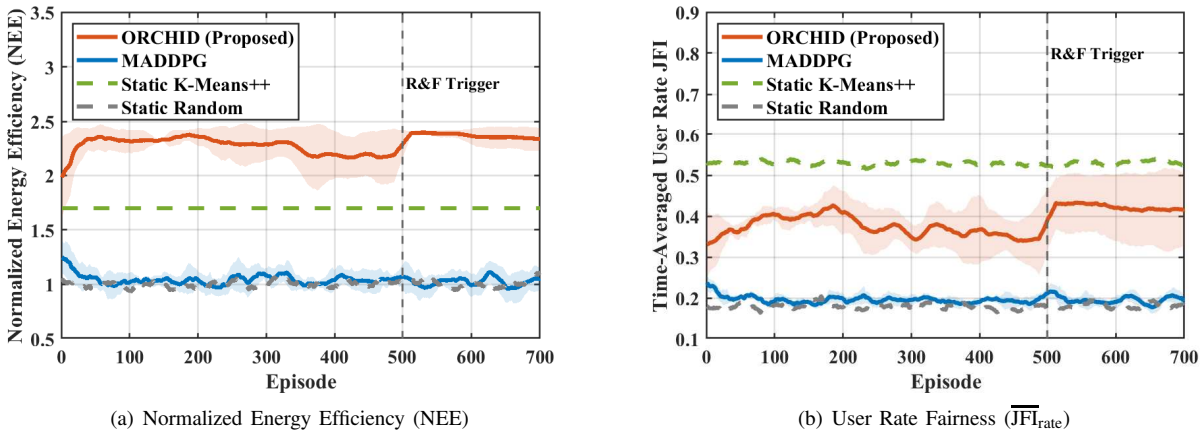


Fig. 4. Comparative analysis of convergence performance against baselines over 700 episodes. The proposed ORCHID demonstrates a significant performance leap following the R&F activation at $e = 500$, while MADDPG exhibits higher variance and lower steady-state efficiency.

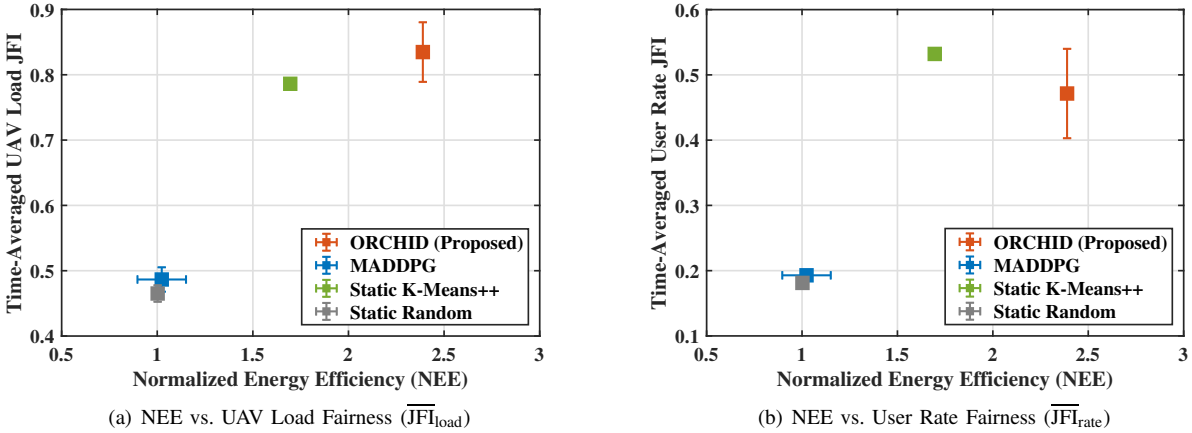


Fig. 5. Performance frontier and trade-off analysis. Each data point is the average of the last 100 episodes across 5 independent runs. ORCHID demonstrates superior Pareto-optimality by simultaneously optimizing system efficiency and service equity.

phase ($e < 500$), the fairness metric fluctuates around 0.35–0.40, struggling to improve further due to the conflicting nature of throughput and fairness objectives. Crucially, the activation of the R&F mechanism at $e = 500$ catalyzes a sharp improvement, elevating the index to a stabilized 0.45. This confirms that the mechanism effectively forces the agents to re-evaluate their greedy strategies and converge towards a solution that better accommodates edge users.

Similarly, the UAV Load JFI (\overline{JFI}_{load} , purple curve) maintains a high level (above 0.8) throughout the process, validating the initial clustering strategy. Post-trigger, it further consolidates to ≈ 0.88 with minimal variance. The synchronous stabilization of all four metrics (Reward, NEE, Rate Fairness, and Load Fairness) after $e = 500$ provides strong empirical evidence that ORCHID's two-stage design effectively resolves the stability-plasticity dilemma in multi-objective MARL.

D. Comparative Analysis

1) *User Coverage Performance*: It is noteworthy that in the considered deployment scenario, all evaluated methods, including the proposed ORCHID framework and the baselines, consistently achieved a near 100% user coverage rate

throughout the episodes. This result is primarily attributed to the sufficient UAV density (6 UAVs per km^2) and the robust link budget maintained by the altitude-aware probabilistic channel model. Since the basic connectivity constraint is satisfied across all schemes, the coverage metric serves as a common reliability baseline, allowing the subsequent performance comparison to focus on the more critical trade-offs between Quality of Service (Normalized EE) and Service Fairness (JFI).

2) *Throughput and Fairness Trade-off*: The comparative performance of ORCHID against three baseline schemes (MADDPG, Static K-Means++, and Static Random) is illustrated in Fig. 4 and Fig. 5.

As shown in Fig. 4(a), while the MADDPG baseline achieves a marginal improvement over the random deployment, its normalized energy efficiency (NEE) remains significantly lower than the proposed ORCHID. This stagnation indicates that standard off-policy RL struggles to escape local optima in high-dimensional continuous action spaces. In contrast, upon the activation of the R&F mechanism at $e = 500$, ORCHID exhibits a distinct performance leap, ultimately achieving the highest NEE among all evaluated

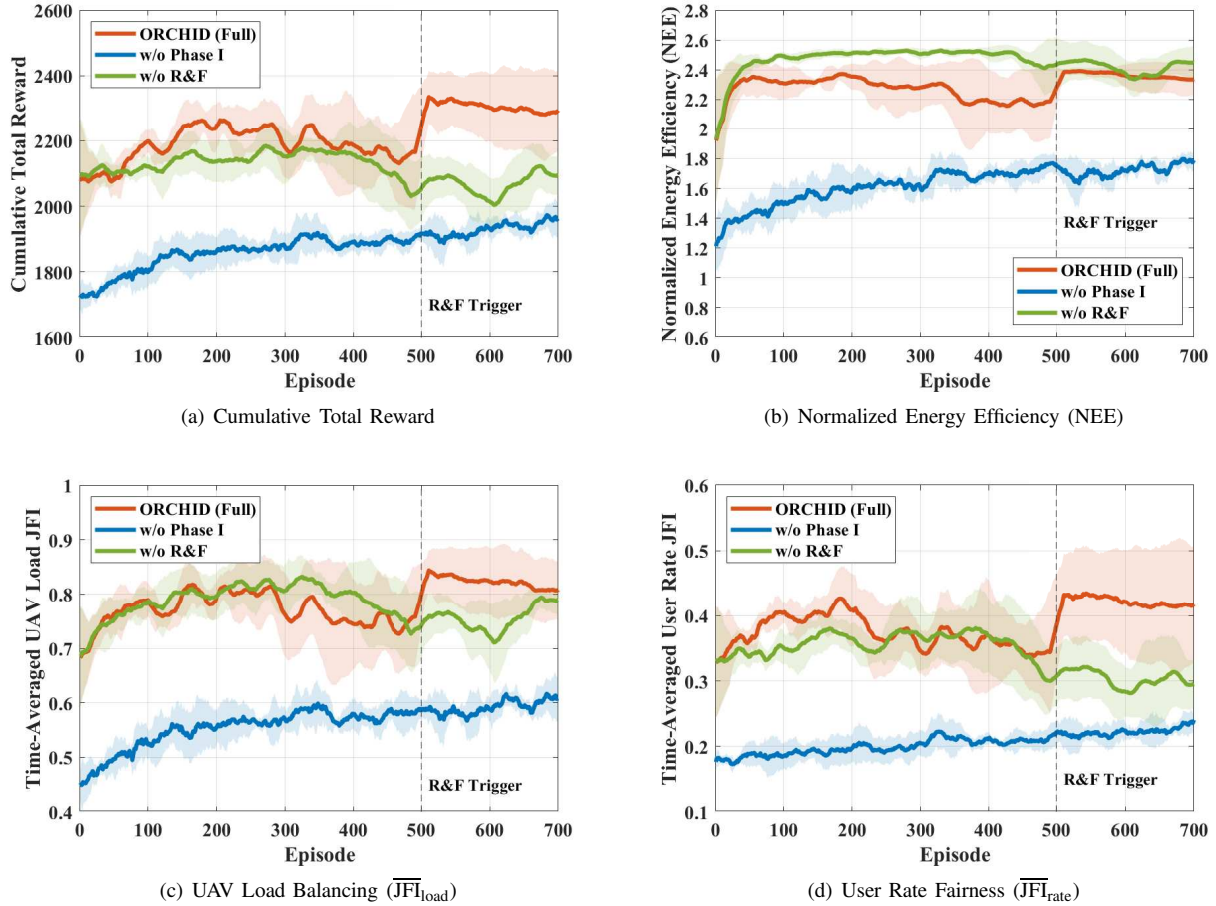


Fig. 6. Comprehensive ablation study of the ORCHID framework over 700 episodes. The vertical dashed line at $e = 500$ denotes the activation of the Reset-and-Finetune (R&F) mechanism. (a) illustrates that the full ORCHID model achieves the highest cumulative reward. (b) reveals that while the variant without R&F (green dashed line) exhibits aggressive growth in NEE, it suffers from severe fluctuations due to the lack of gradient stabilization. (c) and (d) demonstrate that Phase I (K-Means) provides a stable structural floor for load balancing, while the R&F mechanism is essential for locking the system into a high-fairness equilibrium.

schemes. This confirms that the synchronized optimizer reset and learning rate decay ($\eta_{\text{actor}}, \eta_{\text{critic}}$) effectively empower the agents to refine their trajectories for maximizing system efficiency without destabilizing the policy.

The service equity and resource balancing capabilities are further analyzed in Fig. 4(b) and Fig. 5. In Fig. 4(b), the Static K-Means++ baseline exhibits performance fluctuations across episodes, reflecting its sensitivity to the stochastic variations in channel fading and user distribution (TCP) inherent to each simulation run.

The Efficiency-Fairness trade-off is rigorously visualized in Fig. 5. From Fig. 5(a), ORCHID occupies the desired upper-right region, demonstrating its ability to maintain the highest UAV load fairness ($\overline{\text{JFI}}_{\text{load}} \approx 0.9$) while simultaneously maximizing NEE.

Regarding the user rate fairness in Fig. 5(b), a distinct trade-off is observed. Although Static K-Means++ yields the highest $\overline{\text{JFI}}_{\text{rate}}$ due to its rigid geometry-centric partitioning, it suffers from a severe penalty in energy efficiency. This is because static centroids fail to exploit spatial channel diversity, leading to suboptimal spectral efficiency. In contrast, ORCHID maintains a highly competitive fairness level while delivering

the best NEE, confirming its superior Pareto-optimality. By dynamically navigating the efficiency-equity frontier, ORCHID provides a sustainable and balanced service solution suitable for mission-critical emergency communications.

E. Ablation Studies: Impact of Two-Stage Mechanisms

In this subsection, we investigate the contribution of each component within the ORCHID framework to the overall system performance. To verify the necessity of the proposed dual-phase architecture, we compare the full ORCHID framework with two ablated variants:

- 1) **w/o Phase I (Random Init.):** The UAVs are deployed randomly at the start, but the Phase II MARL (with R&F) is retained. This tests the importance of the warm-start initialization.
- 2) **w/o R&F (No Stability Mech.):** The UAVs start from the K-Means centroids, but the Reset-and-Finetune mechanism is removed from Phase II (i.e., standard MAPPO). This tests the importance of the stability enhancement.

To ensure a fair comparison, all variants share the same Max-Min Fairness (MMF) objective and reward structure. The results across four key metrics are illustrated in Fig. 6.

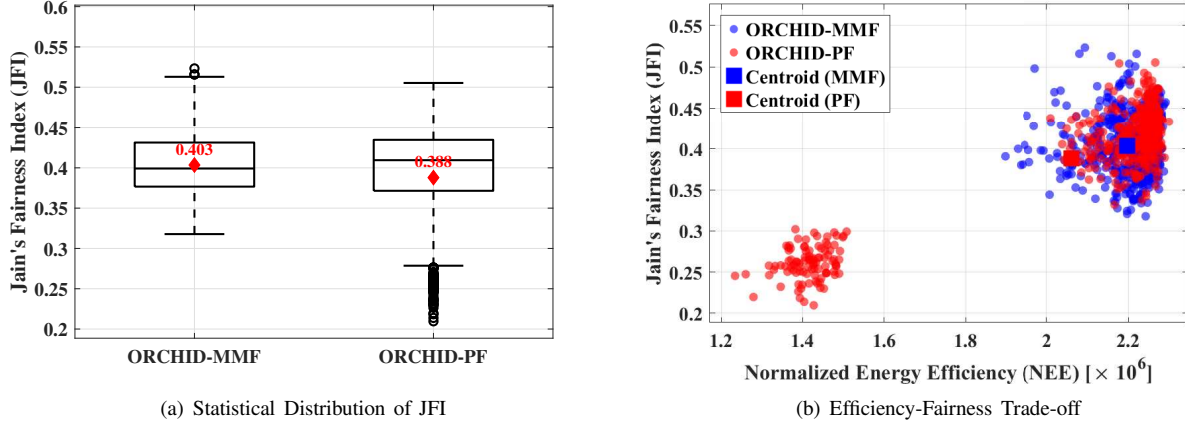


Fig. 7. Comparative strategy analysis between ORCHID-MMF and ORCHID-PF over 5 independent runs. (a) The box plot with diamond markers denotes that MMF achieves a higher mean fairness score (0.403) compared to PF (0.388), verifying its robustness in protecting disadvantaged users. (b) The scatter plot illustrates the **efficiency-fairness synergy**: MMF (blue) shifts towards the upper-right quadrant, simultaneously achieving higher energy efficiency and fairness compared to PF (red), which suffers from suboptimal outliers.

As depicted in Fig. 6(a), the cumulative total reward confirms that the full ORCHID framework achieves the highest overall utility. A critical observation arises from the Normalized Energy Efficiency (NEE) in Fig. 6(b). While the *w/o R&F* variant (green dashed line) exhibits aggressive growth in NEE during early training, it suffers from persistent high-variance fluctuations. This indicates that without the R&F mechanism, agents utilizing the MMF objective tend to oscillate between greedy policies (maximizing throughput for nearby users) and fairness corrections, failing to settle into a sustainable equilibrium.

The critical role of Phase I is evidenced in Fig. 6(c). Without the GBS-aware K-Means initialization (*w/o Phase I*), the UAV load balancing (\overline{JFI}_{load}) remains significantly lower than the proposed method. Notably, the *w/o R&F* variant achieves a similarly high load fairness to the full model, confirming that the spatial workload distribution is primarily governed by the initialization strategy rather than the subsequent fine-tuning. This demonstrates that a structured initial deployment provides a vital performance floor for learning.

In Fig. 6(d), we observe the evolution of user rate fairness. Following the activation of the R&F mechanism at $e = 500$, the full ORCHID model achieves a significantly higher and more stable \overline{JFI}_{rate} compared to the *w/o R&F* variant. Crucially, while the *w/o R&F* variant experiences a performance degradation in fairness after episode 500 (as it greedily pursues NEE), the R&F mechanism effectively reverses this trend. This demonstrates that R&F is essential for solving the inherent instability of the MMF objective. Without this stabilization phase (Optimizer Reset and Decay), the gradient noise causes the policy to drift away from the fairness-optimal solution. By suppressing this noise, R&F allows the UAVs to fine-tune their trajectories to satisfy the minimum rate requirements of the most disadvantaged users.

This design choice highlights ORCHID's suitability for mission-critical scenarios, where ensuring service equity for all ground users is as essential as maintaining the energy efficiency of the UAV fleet.

F. Strategy Analysis: Efficiency-Fairness Synergy

To rigorously validate the adaptability of ORCHID in mission-critical scenarios, we conducted a comparative analysis between the proposed Max-Min Fairness (MMF) strategy and the standard Proportional Fairness (PF) scheme. To ensure statistical reliability given the stochastic nature of DRL, we performed 5 independent runs for each strategy and aggregated the performance metrics over the final 100 convergence episodes.

Fig. 7 presents the comprehensive analysis results. In Fig. 7(a), the box plot distribution reveals that the ORCHID-MMF strategy achieves a superior mean user fairness ($\overline{JFI}_{rate} \approx 0.403$) compared to the PF variant (≈ 0.388). This represents a statistically significant gain of approximately 3.86%. Unlike PF, which tends to sacrifice cell-edge users to maximize aggregate metrics (evidenced by the lower outliers), the MMF objective consistently enforces a “no-user-left-behind” policy, pushing the system equilibrium toward a more equitable state as evidenced by the tighter interquartile range (IQR).

More remarkably, the efficiency analysis visualized in Fig. 7(b) uncovers a counter-intuitive *efficiency-fairness synergy*. Contrary to the conventional wisdom where fairness comes at the cost of spectral efficiency, our results indicate that ORCHID-MMF outperforms PF in Normalized Energy Efficiency (NEE) by a notable margin of 6.8% (MMF: $\approx 2.20 \times 10^6$ vs. PF: $\approx 2.06 \times 10^6$). The scatter plot demonstrates that while PF clusters are dispersed in the lower-efficiency region, the MMF solutions (blue) shift decisively toward the upper-right quadrant, dominating PF in both dimensions. This phenomenon suggests that the greedy nature of PF leads to suboptimal local equilibria, likely characterized by inefficient spatial deployment or excessive path loss attenuation in complex topologies. In contrast, ORCHID-MMF promotes a globally coordinated constellation that is both fairer and more energy-efficient. Thus, MMF proves to be the robust strategic choice for mission-critical AGINs, delivering high-quality service without compromise.

VI. CONCLUSION

In this paper, we proposed ORCHID, a resilient two-stage orchestration framework designed to optimize collaborative UAV-GBS deployment in mission-critical air-ground integrated networks (AGINs). By synergizing GBS-aware topology partitioning with a MAPPO-based Reset-and-Finetune (R&F) mechanism, the framework effectively resolves the stability-plasticity dilemma inherent in multi-objective MARL. Our comprehensive strategy analysis reveals a counter-intuitive yet critical design insight: contrary to the conventional efficiency-fairness trade-off, the proposed MMF-driven approach acts as a strategic efficiency-fairness synergy. Simulation results confirm that ORCHID-MMF not only secures a robust “no-user-left-behind” service equity but also achieves a 6.8% higher Normalized Energy Efficiency (NEE) compared to the standard Proportional Fairness (PF) scheme. This finding overturns the assumption that fairness must come at the cost of spectral efficiency, demonstrating that the greedy nature of PF leads to suboptimal local equilibria in complex spatial topologies.

Overall, ORCHID establishes a Pareto-dominant position against state-of-the-art baselines (e.g., MADDPG) and static heuristics. Future work will extend this framework to high-mobility vehicular environments, exploring the integration of Integrated Sensing and Communication (ISAC) protocols and decentralized onboard inference to further enhance the resilience of next-generation emergency networks.

REFERENCES

- [1] Z. Jia, C. Cui, C. Dong, Q. Wu, Z. Ling, D. Niyato, and Z. Han, “Distributionally robust optimization for aerial multi-access edge computing via cooperation of uavs and hasps,” *IEEE Transactions on Mobile Computing*, vol. 24, no. 10, pp. 10 853–10 867, 2025.
- [2] W. Zhao, S. Cui, W. Qiu, Z. He, Z. Liu, X. Zheng, B. Mao, and N. Kato, “A survey on drl-based uav communications and networking: Drl fundamentals, applications and implementations,” *IEEE Communications Surveys & Tutorials*, vol. 28, pp. 3911–3941, 2026.
- [3] Q. Chen, Z. Guo, W. Meng, S. Han, C. Li, and T. Q. S. Quek, “A survey on resource management in joint communication and computing-embedded sagin,” *IEEE Communications Surveys & Tutorials*, vol. 27, no. 3, pp. 1911–1954, 2025.
- [4] M. Giordani and M. Zorzi, “Non-terrestrial networks in the 6g era: Challenges and opportunities,” *IEEE Network*, vol. 35, no. 2, pp. 244–251, 2021.
- [5] C. Zhan, W. Liu, K. Song, R. Fan, J. Liu, and H. Hu, “Joint uav placement and dependent task offloading in multi-uav mec networks: a graph attention enhanced drl approach,” *IEEE Transactions on Mobile Computing*, pp. 1–17, 2025.
- [6] Y. Zeng, R. Zhang, and T. J. Lim, “Wireless communications with unmanned aerial vehicles: opportunities and challenges,” *IEEE Communications Magazine*, vol. 54, no. 5, pp. 36–42, 2016.
- [7] C.-C. Lai, L.-C. Wang, and Z. Han, “The coverage overlapping problem of serving arbitrary crowds in 3d drone cellular networks,” *IEEE Transactions on Mobile Computing*, vol. 21, no. 3, 2022.
- [8] C.-C. Lai, C.-T. Chen, and L.-C. Wang, “On-demand density-aware uav base station 3d placement for arbitrarily distributed users with guaranteed data rates,” *IEEE Wireless Communications Letters*, vol. 8, no. 3, pp. 913–916, 2019.
- [9] A. Mahmood, T. X. Vu, S. Chatzinotas, and B. Ottersten, “Joint optimization of 3d placement and radio resource allocation for per-uav sum rate maximization,” *IEEE Transactions on Vehicular Technology*, vol. 72, no. 10, pp. 13 094–13 105, 2023.
- [10] C.-C. Lai, Bhola, A.-H. Tsai, and L.-C. Wang, “Adaptive and fair deployment approach to balance offload traffic in multi-uav cellular networks,” *IEEE Transactions on Vehicular Technology*, vol. 72, no. 3, pp. 3724–3738, 2023.
- [11] R. Jain, D.-M. Chiu, and W. Hawe, “A quantitative measure of fairness and discrimination for resource allocation in shared systems,” digital equipment corporation,” Technical Report DEC-TR-301, Tech. Rep., 1984.
- [12] D. Wei, L. Zhang, Q. Liu, H. Chen, and J. Huang, “Uav swarm cooperative dynamic target search: A mappo-based discrete optimal control method,” *Drones*, vol. 8, no. 6, 2024.
- [13] R. Lowe, Y. Wu, A. Tamar, J. Harb, P. Abbeel, and I. Mordatch, “Multi-agent actor-critic for mixed cooperative-competitive environments,” in *Proceedings of the 31st International Conference on Neural Information Processing Systems*, Long Beach, California, USA, 2017, pp. 6382–6393.
- [14] C. Yu, A. Velu, E. Vinitsky, J. Gao, Y. Wang, A. Bayen, and Y. Wu, “The surprising effectiveness of ppo in cooperative multi-agent games,” in *Proceedings of the 36th International Conference on Neural Information Processing Systems*, New Orleans, LA, USA, 2022.
- [15] D. Arthur and S. Vassilvitskii, “k-means++: the advantages of careful seeding,” in *Proceedings of the Eighteenth Annual ACM-SIAM Symposium on Discrete Algorithms*, New Orleans, Louisiana, 2007, pp. 1027–1035.
- [16] M. Mozaffari, W. Saad, M. Bennis, and M. Debbah, “Efficient deployment of multiple unmanned aerial vehicles for optimal wireless coverage,” *IEEE Communications Letters*, vol. 20, no. 8, pp. 1647–1650, 2016.
- [17] D. K. R. and R. A., “Optimizing uav deployment for maximizing coverage and data rate efficiency using multi-agent deep deterministic policy gradient and bayesian optimization,” *Physical Communication*, vol. 69, p. 102621, 2025.
- [18] S. Swain, R. Ranjan Swain, B. Ranjan Senapati, and P. Mohan Khilar, “An optimized 2d ground area coverage using uav-enabled sensor networks,” *IEEE Access*, vol. 13, pp. 161 299–161 310, 2025.
- [19] J. Qin, Z. Wei, C. Qiu, and Z. Feng, “Edge-prior placement algorithm for uav-mounted base stations,” in *2019 IEEE Wireless Communications and Networking Conference (WCNC)*, 2019, pp. 1–6.
- [20] G. Zhang, Q. Wu, M. Cui, and R. Zhang, “Securing uav communications via joint trajectory and power control,” *IEEE Transactions on Wireless Communications*, vol. 18, no. 2, pp. 1376–1389, 2019.
- [21] J. Lei, T. Zhang, X. Mu, and Y. Liu, “Noma for star-ris assisted uav networks,” *IEEE Transactions on Communications*, vol. 72, no. 3, pp. 1732–1745, 2024.
- [22] X. Li, Q. Wang, Y. Liu, T. A. Tsiftsis, Z. Ding, and A. Nallanathan, “Uav-aided multi-way noma networks with residual hardware impairments,” *IEEE Wireless Communications Letters*, vol. 9, no. 9, pp. 1538–1542, 2020.
- [23] C. H. Liu, X. Ma, X. Gao, and J. Tang, “Distributed energy-efficient multi-uav navigation for long-term communication coverage by deep reinforcement learning,” *IEEE Transactions on Mobile Computing*, vol. 19, no. 6, pp. 1274–1285, 2020.
- [24] J. Hu, H. Zhang, L. Song, R. Schober, and H. V. Poor, “Cooperative internet of uavs: Distributed trajectory design by multi-agent deep reinforcement learning,” *IEEE Transactions on Communications*, vol. 68, no. 11, pp. 6807–6821, 2020.
- [25] Z. Ning, Y. Yang, X. Wang, Q. Song, L. Guo, and A. Jamalipour, “Multi-agent deep reinforcement learning based uav trajectory optimization for differentiated services,” *IEEE Transactions on Mobile Computing*, vol. 23, no. 5, pp. 5818–5834, 2024.
- [26] H. Kang, X. Chang, J. Mišić, V. B. Mišić, J. Fan, and Y. Liu, “Cooperative uav resource allocation and task offloading in hierarchical aerial computing systems: A mappo-based approach,” *IEEE Internet of Things Journal*, vol. 10, no. 12, pp. 10 497–10 509, 2023.
- [27] S. Fu, X. Feng, A. Sultana, and L. Zhao, “Joint power allocation and 3d deployment for uav-bss: A game theory based deep reinforcement learning approach,” *IEEE Transactions on Wireless Communications*, vol. 23, no. 1, pp. 736–748, 2024.
- [28] M. Zhao, W. Li, L. Bao, J. Luo, Z. He, and D. Liu, “Fairness-aware task scheduling and resource allocation in uav-enabled mobile edge computing networks,” *IEEE Transactions on Green Communications and Networking*, vol. 5, no. 4, pp. 2174–2187, 2021.
- [29] S. N. Chiu, D. Stoyan, W. S. Kendall, and J. Mecke, *Stochastic Geometry and its Applications*. John Wiley & Sons, 2013.
- [30] A. Al-Hourani, S. Kandeepan, and S. Lardner, “Optimal lap altitude for maximum coverage,” *IEEE Wireless Communications Letters*, vol. 3, no. 6, pp. 569–572, 2014.
- [31] G. Papoudakis, F. Christianos, A. Rahman, and S. V. Albrecht, “Dealing with non-stationarity in multi-agent deep reinforcement learning,” 2019. [Online]. Available: <https://arxiv.org/abs/1906.04737>

- [32] E. Nikishin, M. Schwarzer, P. D’Oro, P.-L. Bacon, and A. Courville, “The primacy bias in deep reinforcement learning,” in *International Conference on Machine Learning (ICML)*, Baltimore, Maryland, USA, 2022.
- [33] J. T. Ash and R. P. Adams, “On warm-starting neural network training,” in *International Conference on Neural Information Processing Systems (NIPS)*, Vancouver, BC, Canada, 2020.
- [34] S. J. Reddi, S. Kale, and S. Kumar, “On the convergence of adam and beyond,” in *International Conference on Learning Representations (ICLR)*, Vancouver, BC, Canada, 2018.



Chuan-Chi Lai (Member, IEEE) received the Ph.D. degree in Computer Science and Information Engineering from National Taipei University of Technology, Taipei, Taiwan, in 2017. He was a postdoctoral research fellow (2017–2019) and contract assistant research fellow (2020) with the Department of Electrical and Computer Engineering, National Chiao Tung University, Hsinchu, Taiwan. From Feb. 2021 to Jan. 2024, he served as an assistant professor at the Department of Information Engineering and Computer Science, Feng Chia University, Taichung, Taiwan.

From Feb. 2024, he is currently an assistant professor at the Department of Communications Engineering, National Chung Cheng University, Chiayi, Taiwan. He is a member of the IEEE Computer Society, IEEE Communications Society, and IEEE Vehicular Technology Society. His research interests include resource allocation, data management, information dissemination, and distributed query processing for moving objects in emerging applications such as the Internet of Things, edge computing, and next-generation wireless networks. Dr. Lai received the Postdoctoral Researcher Academic Research Award from the Ministry of Science and Technology, Taiwan, in 2019, Best Paper Awards at WOCC 2021 and WOCC 2018, and the Excellent Paper Award at ICUFN 2015.



Chi Jai Choy received the B.S. degree in Computer Science and Information Engineering from Feng Chia University, Taichung, Taiwan, in 2021, and the M.S. degree in Computer Science and Information Engineering from Feng Chia University, Taichung, Taiwan, in 2025. His research interests include multi-agent reinforcement learning, UAV-enabled communications, and energy-efficient wireless networks.